

# Combining Effect of Er and Sr on Microstructure and Mechanical Properties of As-casted A356 Alloy

Chen Zhiqiang<sup>1,2</sup>, Jia Jinyu<sup>2</sup>, Hu Wenxin<sup>1,2</sup>, Wang Wei<sup>2</sup>, Wang Xiaoqing<sup>1,2</sup>

<sup>1</sup> State Key Laboratory of Baiyunobo Rare Earth Resource Researches and Comprehensive Utilization, Baotou Research Institute of Rare Earths, Baotou 014030, China; <sup>2</sup> Baotou Research Institute of Rare Earths, Baotou 014030, China

**Abstract:** In order to investigate the combining effect of Er and Sr on the microstructure and mechanical properties of A356 alloy, Al-10Er-5Sr master alloy was fabricated and its microstructure and phase compositions were investigated. The optimal content of Al-10Er-5Sr in A356 alloy was obtained according to the evolution of microstructure and mechanical properties. The results show that  $\alpha$ -Al, Al<sub>4</sub>Sr and Al<sub>3</sub>Er are the main phases in Al-10Er-5Sr. In addition, the aluminum alloy with 0.6wt% Al-10Er-5Sr exhibits optimal microstructure and mechanical properties, with the secondary dendrite arm spacing (SDAS) decreasing to 20.2  $\mu$ m and acicular-like eutectic silicon transforming to fibrous. Due to the improved microstructure, the ultimate tensile strength of the alloy (with 0.6wt% Al-10Er-5Sr) increases to 203.5 MPa, which is much better than that of untreated A356 aluminum alloy. Finally, the grain refinement and modification mechanisms were discussed.

**Key words:** Al-10Er-5Sr master alloy; modification and grain refinement; combining effect; mechanical properties

The A356 aluminum alloy has widespread applications especially in the aerospace and automotive industries because of the excellent properties including castability, weldability, corrosion resistance and integrated mechanical properties<sup>[1,2]</sup>. While, as it is well known, the tensile strength and ductility of the as-cast alloy are limited by the coarse dendritic structures and acicular-like eutectic silicon phase<sup>[3,4]</sup>. To improve mechanical properties, in particular to increase the tensile elongation, the modification of the coarse eutectic phase can be achieved in various ways, such as adding certain elements (chemical modification), a rapid cooling rate (quench modification), semi-solid processing and electromagnetic stirring<sup>[5-10]</sup>. It is found that adding element is the most popular and effective. The eutectic silicon phase is usually modified from coarse and plate-like to fine and fibrous morphology by adding the elements such as strontium (Sr), sodium (Na), antimony (Sb) and rare earth elements to the melt<sup>[11,12]</sup>. Specifically, Sr and its master alloys, as a kind of the most effective modifiers, were extensively investigated and used<sup>[13,14]</sup>. Emamy et al<sup>[15]</sup> found that the optimal Sr level for

introducing a uniform structure was 0.2wt% in A356-10% B<sub>4</sub>C metal matrix composite, while the Sr addition did not change tensile results significantly but the elongation enhancement was meaningful. Cui et al<sup>[16]</sup> found that 0.5wt% Al-3B-5Sr master alloy produced satisfactory grain refining and modifying effects, resulting in the improved mechanical properties of A356 alloy. Similar effect was obtained by the addition of Al-Ti-C-Sr into A356 alloy<sup>[17]</sup>. Among rare earth elements, Er proved to be an effective strengthening element for Al alloys<sup>[18-20]</sup>. Recent studies have focused on the addition of Er to Al-Si-Mg-(Cu) hypoeutectic or eutectic alloys<sup>[21,22]</sup>, showing improved yield stress (YS), ultimate tensile strength (UTS) and elongation to fracture ( $\delta\%$ ) of Er containing alloys after room temperature tensile tests. The effect of Er can be explained by the precipitation of nanometric Li<sub>2</sub>Al<sub>3</sub>Er dispersoids that, due to their crystallographic coherency with Al and their low coarsening rates, are very effective in retarding dislocations motions. It can be seen from the reported literatures that the effect of Sr and Er elements on A356 alloy was investigated individually. Meanwhile, it is

Received date: October 20, 2019

Foundation item: National Key Research and Development Program (2016YFB0101205)

Corresponding author: Chen Zhiqiang, Master, Baotou Research Institute of Rare Earths, Baotou 014030, P. R. China, Tel: 0086-472-5179599, E-mail: 632330923@qq.com

Copyright © 2020, Northwest Institute for Nonferrous Metal Research. Published by Science Press. All rights reserved.

assumed that a proper coordination of Sr and Er can have a good grain refinement and modification effect on A356 alloy. However, to our best knowledge, few literatures have reported the actual experimental data up to date. Therefore, it is necessary to investigate the synergistic effect of Sr and Er on the microstructure and mechanical properties of A356 alloy.

In this work, the microstructure and phase compositions of Al-10Er-5Sr master alloy were investigated. What's more, the influence of Al-10Er-5Sr on the microstructure and tensile properties of the as-casted A356 aluminum alloy were studied and the optimal content was obtained. Meanwhile, the mechanisms of the synergistic effect of Sr and Er addition on the grain refinement and eutectic modification in hypoeutectic Al-Si alloy were discussed.

## 1 Experiment

In this experiment, pure aluminum (with the purity of 99.7%), binary Al-10Sr and Al-10Er master alloys were used for preparation of Al-10Er-5Sr master alloy. Detailed steps were as follows: Firstly, melting pure aluminum at the temperature of 740 °C in an induction melting furnace and holding the melt for 10 min. Secondly, removing the slag, raising the temperature to 800 °C and holding for 10 min. Thirdly, adding Al-10Sr and Al-10Er master alloys into the melt and holding for 15 min, then stirring the melt for 5 min. Finally, reducing the temperature to 720 °C and keeping for 10 min, then pouring the melt into a permanent mold to obtain Al-10Er-5Sr master alloy.

A356 alloys with different contents (0.0wt%, 0.4wt%, 0.6wt%, 0.8wt%, 1.0wt%) of Al-10Er-5Sr were prepared as follows: First, melting about 1000 g of A356 alloy in a graphite crucible with a well electric resistance furnace at the temperature of 750 °C, removing the slag and degassing the melt by flowing high purity argon gas for 5 min. Second, adding certain quantity of Al-10Er-5Sr master alloy (with the compositions shown in Table 1) into the melt, holding for 10 min and degassing the melt again for 5 min. At last, removing the slag and pouring the melt into a permanent mold (the inner diameter and height of 45 mm and 160 mm, respectively) to obtain the required specimens.

To ensure the reproducibility of the experiment, samples used for microstructure observation were cut into the dimensions of 10 mm×10 mm×10 mm by an electro-discharging machine from the same position of the specimens. Typical metallographic method was applied for sample preparation. Namely, samples were gradually prepared by grinding through 400#, 600#, 800#, 1000#, 1500# and 2000# grit papers followed by polishing with 0.5 μm polishing paste, then the samples were

etched by Keller's reagent for 15 s at room temperature, finally rinsed with distilled water, alcohol and dried by cold flowing air. Olymups-BX41M optical-microscope (OM) and Hitachi S4800 scanning electron microscope (SEM) equipped with energy-dispersive spectra (EDS) were used for microstructure observation. SmartLab (Rigaku) X-ray diffraction (XRD) using copper K $\alpha$  radiation was employed to identify the phase compositions. Image Pro Plus 6.0 software was applied to measure the grain distribution, secondary dendrite arm spacing (SDAS) and the morphology of eutectic silicon.

Tensile properties (according to the standard of GB/T228.1-2010) of the samples were obtained at room temperature by using a SANS Electron Universal Material Testing Machine, with a maximum load of 10 kN. The tests were controlled by a displacement speed of 0.5 mm/min and the results were recorded by a personal computer. For each condition more than three samples were tested to guarantee the reproducibility and the average values were used in this paper.

## 2 Results and Discussion

### 2.1 Microstructure and phase composition of Al-10Er-5Sr master alloy

The chemical composition of Al-10Er-5Sr master alloys is very close to the designed composition, as shown in Table 1. The microstructure of Al-10Er-5Sr master alloy is displayed in Fig.1. It can be seen that the white block phases, the dark strip-like phases and lots of acicular phases (the length and width of about 30 μm and 0.5~1 μm, respectively) are embedded in the matrix, as shown in Fig.1a. The EDS results shown in Fig.1b and 1c indicate that the atomic ratio of Al:Er is around 4:1, which means that the dark strip-like phases can be regarded as Al<sub>4</sub>Er. The EDS result shown in Fig.1d indicates that the white block phase is AlEr intermediate compound. To clearly clarify the phase compositions, XRD detection was applied and the result is shown in Fig.2. It can be proved that Al-10Er-5Sr master alloy is mainly composed of  $\alpha$ -Al, Al<sub>4</sub>Er and Al<sub>3</sub>Er phases.

### 2.2 Grain refinement and modification performance of Al-10Er-5Sr

The grain refinement, modification performance and SDAS evolutions of A356 alloy treated by the Al-10Er-5Sr are presented in Fig.3 and Fig.4, respectively. It can be seen that the phase composition of the untreated A356 alloy is composed of the coarse  $\alpha$ -Al dendrites and acicular-like eutectic silicon, as shown in Fig.3a. The SDAS of the untreated A356 alloy is about 36.1 μm. It is clear that the sample with small quantities of Al-10Er-5Sr (0.4wt%, as shown in Fig.3b and Fig.4), the morphology of eutectic silicon transforms from acicular-like to fibrous and the SDAS decreases to 25.56 μm. In addition, with increasing the Al-10Er-5Sr content to 0.6wt% (as shown in Fig.3c), the content of the coarse dendrites decreases obviously and more equiaxed crystals form. Additionally, the SDAS significantly decreases to 20.2 μm,

**Table 1 Chemical compositions of Al-10Er-5Sr master alloys (wt%)**

Er	Sr	Al
9.52	4.68	Bal.

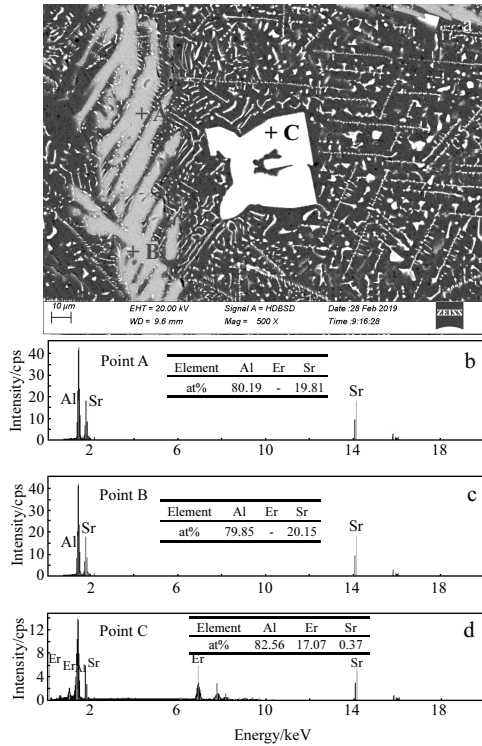


Fig.1 SEM microstructure (a) and EDS results of points A (b), B (c), C (d) of Al-10Er-5Sr master alloy in Fig.1a

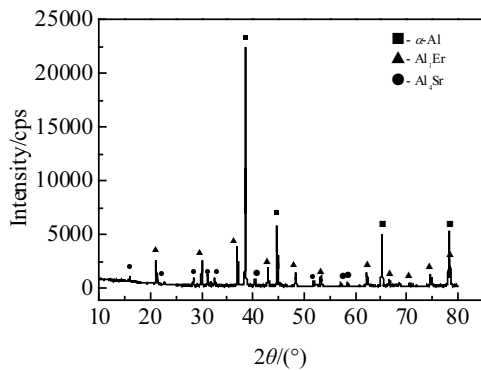


Fig.2 Phase composition of Al-10Er-5Sr master alloy

which is about 56% of that of the untreated alloy. The grains are apparently refined. With increasing the Al-10Er-5Sr content to 0.8wt%, the equiaxed crystals coarsen and the coarse dendrites increase, as shown in Fig.3d. The SDAS slightly increases to about 24.3  $\mu\text{m}$ . With increasing the Al-10Er-5Sr content to 1.0wt% (as shown in Fig.3e), the coarse dendritic structures decrease slightly and the SDAS reach 23.96  $\mu\text{m}$ . Under the present conditions, specimens with Al-10Er-5Sr content of 0.6wt% possess the optimal grain refinement performance.

In order to further understand the effect of Al-10Er-5Sr, more detailed detections and analyses are applied. Fig.5 shows

the morphology evolution of eutectic silicon treated by different processes. Acicular-like eutectic silicon with the length of 20~50  $\mu\text{m}$  and width of 2~5  $\mu\text{m}$  are found in the untreated A356 alloy (Fig.5a). Meanwhile, some blocky eutectic silicon of 5~7  $\mu\text{m}$  are also embedded in the matrix. For the alloy treated with 0.4wt% Al-10Er-5Sr (Fig.5b) acicular-like eutectic silicon changes into fibrous with the length of 1~5  $\mu\text{m}$ . While, it should be noted that some irregular blocky eutectic silicon of 5~7  $\mu\text{m}$  can still be found, which may deteriorate the as-cast mechanical properties of A356 aluminum alloy. For the alloy treated with 0.6wt% Al-10Er-5Sr (Fig.5c) almost all of the eutectic silicon are short fibrous or fine particles of 1~2  $\mu\text{m}$  which homogeneously distribute along the grain boundaries. When the addition of Al-10Er-5Sr reaches 0.8wt%, the modified eutectic silicon in Fig.5d is slightly inferior to the one in Fig.5b. However, the 1.0wt% addition of Al-10Er-5Sr in turn coarsens the eutectic silicon.

### 2.3 Mechanical performance of A356 with Al-10Er-5Sr

Fig.6 shows the mechanical properties of A356 alloy with different treating processes. It is clear that the ultimate tensile strength of the specimens increases first and then decreases gradually. The tensile strength of the untreated alloy is 183.9 MPa. As for the alloys treated by Al-10Er-5Sr master alloy (as shown in Fig.6), the mechanical properties increase gradually as the content of Al-10Er-5Sr increases from 0.0wt% to 0.6wt%. Particularly, the alloy with the Al-10Er-5Sr content of 0.6wt% possesses the highest ultimate tensile strength (up to 203.5 MPa), which is improved by 10.7% compared with the untreated alloy. When the addition of the Al-10Er-5Sr master alloy reaches 0.8 wt% or more, the tensile strength decreases gradually. Compared with A356 alloys treated by different contents of master alloys<sup>[21,23-25]</sup>, an excellent increment of strength performance can be achieved by addition of Al-10Er-5Sr master alloy (as shown in Table 2).

### 2.4 Discussion

#### 2.4.1 Effect of Al-10Er-5Sr alloy on the refinement of $\alpha$ -Al grains

Grain refinement process of Al-10Er-5Sr master alloy can be explained as follows: Al-10Er-5Sr is added in the form of master alloy and it is composed of  $\alpha$ -Al, Al<sub>4</sub>Sr and Al<sub>3</sub>Er phases (as shown in Fig.2). Thus, during the solidification of the melt, Al<sub>4</sub>Sr (with melting point of 1025  $^{\circ}\text{C}$ ) and Al<sub>3</sub>Er (with melting point of 1070  $^{\circ}\text{C}$ ) can stably exist in the melt and the lattice constants of Al<sub>4</sub>Sr and Al<sub>3</sub>Er are similar to  $\alpha$ -Al, so they can be served as the nucleating sites for  $\alpha$ -Al<sup>[26,27]</sup>, leading to heterogeneous nucleation of  $\alpha$ -Al and refined  $\alpha$ -Al (as shown in Fig.3). It has been known that SDAS is one of the critical parameters of dendrite structure, which reflects the refinement effect of a refiner. Meanwhile, smaller SDAS can result in the reduction of elements segregation and microporosities, leading to the improvement of mechanical properties<sup>[28]</sup>. In addition, SDAS is determined by the growth and ripening

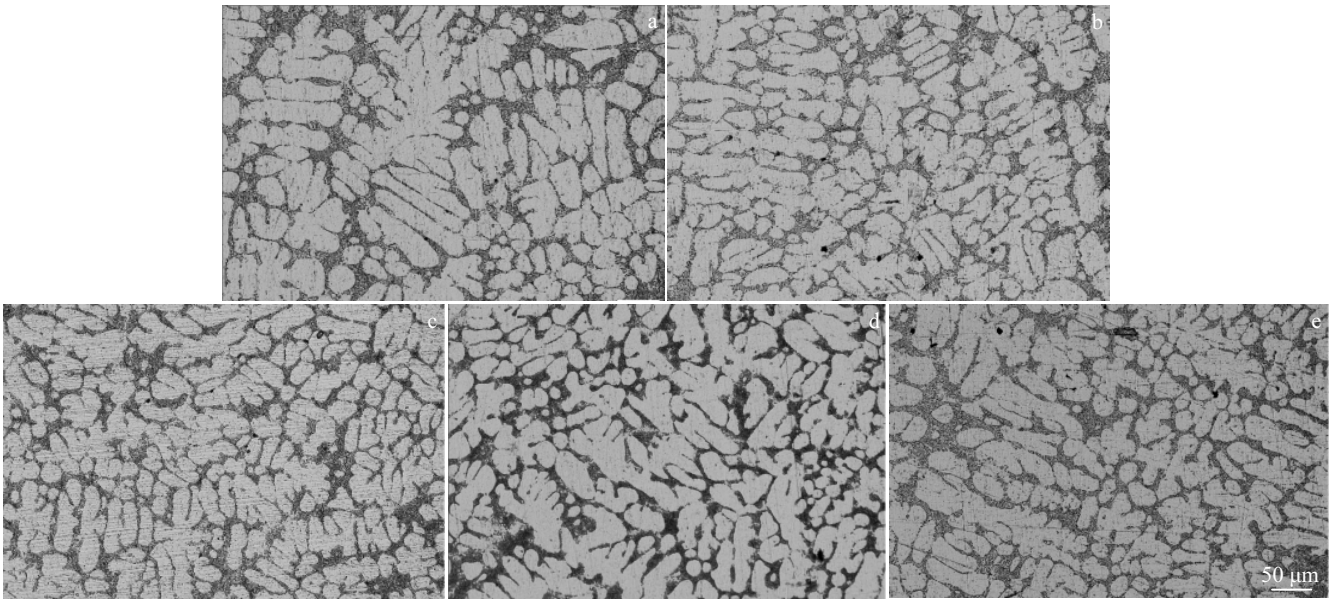


Fig.3 Microstructures of A356 alloys with different contents of Al-10Er-5Sr: (a) 0.0wt%, (b) 0.4wt%, (c) 0.6wt%, (d) 0.8wt%, and (e) 1.0wt%

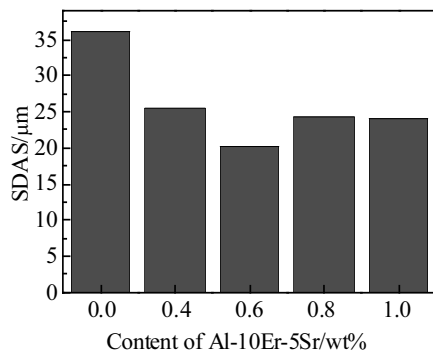


Fig.4 SDAS evolution of A356 alloys with different contents of Al-10Er-5Sr

process of secondary dendrites. Once the diffusion field of one dendritic crystal contact with the field of another, they begin to ripen and coarsen. In the present conditions, the 0.6wt% Al-10Er-5Sr addition achieves the smallest SDAS value, which notes the alloy treated by 0.6wt% Al-10Er-5Sr achieves the best effect on the  $\alpha$ -Al grain refinement. The refining effect was also found in the literature<sup>[21-23]</sup>.

On the other hand, increasing the Al-10Er-5Sr content ( $\geq 0.8$ wt%) in turn reduces the refinement effect. This reduction can be ascribed to the formation of AlSiMgEr and AlSiMg-FeSrEr intermetallic compounds (as shown in Fig.7 and Table 3), resulting in the loss of the Si and Mg solutes, leading to the deviation of the alloy composition from that of Er-free composites, which will increase the SDAS value. The similar

phenomenon was also identified in the literature<sup>[20,22,23]</sup>.

#### 2.4.2 Effect of the Al-10Er-5Sr alloy on the refinement of silicon phases

In order to identify the modification mechanism of Al-10Er-5Sr, area scanning was used and the distribution of the concerned elements (Al, Si, Sr, Er) are displayed in Fig.8. It is confirmed that Si and Sr are obviously segregated on the grain boundary and the segregation path of Sr is consistent with that of Si, while Er distributes homogeneously in the matrix. It is illustrated that the modification mechanism of Sr is that Sr-rich compounds partly dissolve and release Sr atoms<sup>[16]</sup>, then Sr atoms accumulate at the solid-liquid interface and are absorbed in the Si lattice, leading to the poison of the {111} closely packed planes in Si. Thus, the frequent twinning is promoted and the growth rate of Si phases is reduced and the growth flexibility of the Si branches is accelerated correspondingly. As a consequence, the modified eutectic Si is prone to bend, curve and split, leading to the finer morphology of eutectic Si<sup>[21]</sup>. As the Er atom has a smaller atomic radius (0.175 nm) and a large atomic mass (167.26) than the Sr atom (0.215 nm, 87.62), it is easier to enrich in front of the eutectic cells because of its difficulty in diffusion, which greatly poisons the orientation growth of the Si phases. Moreover, the Er atom has a more physicochemical activity than Sr, La and Ce atoms, which can eliminate the oxide bifilms and purify the melts. With these two reasons, the fine particles or short rods form. A similar phenomenon was also found in the Er-modified Al-12.6wt% Si hypereutectic alloys, but the action mechanism was not provided<sup>[22,29]</sup>. Above all, the satisfactory grain refinement and modification perfor-

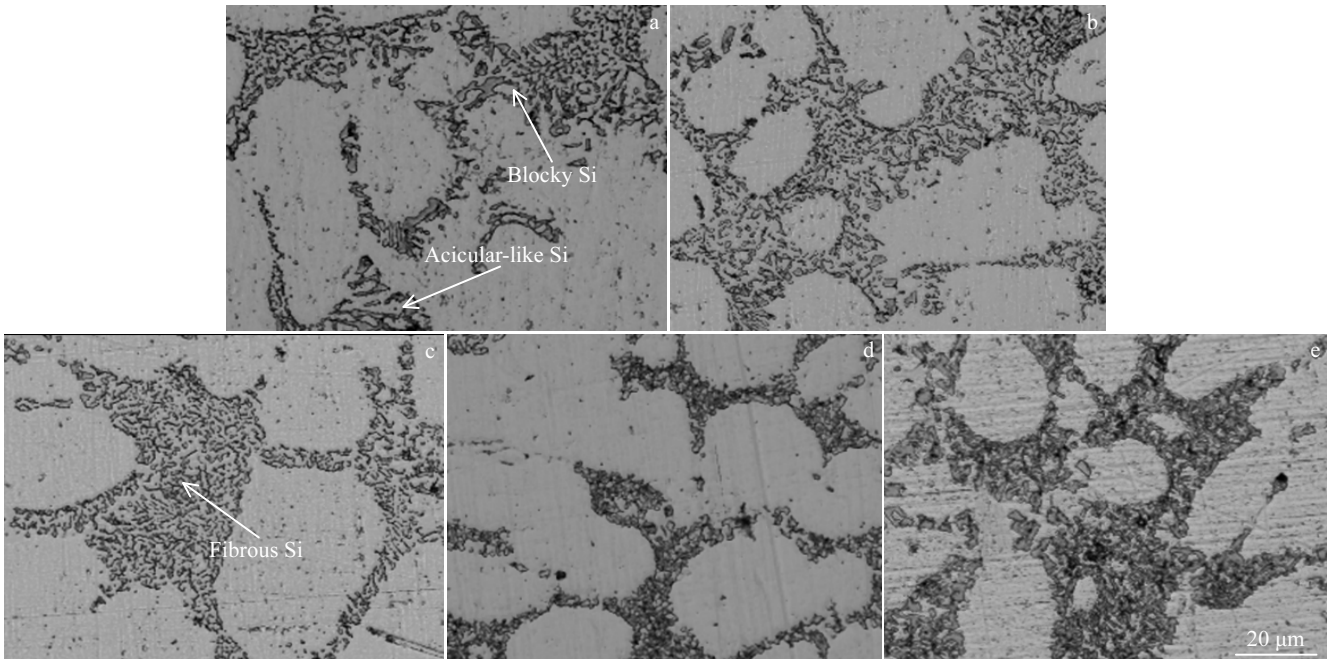


Fig.5 Morphologies of eutectic silicon particles of modified A356 alloys with different contents of Al-10Er-5Sr at T6 state: (a) 0.0wt%, (b) 0.4wt%, (c) 0.6wt%, (d) 0.8wt%, and (e) 1.0wt%

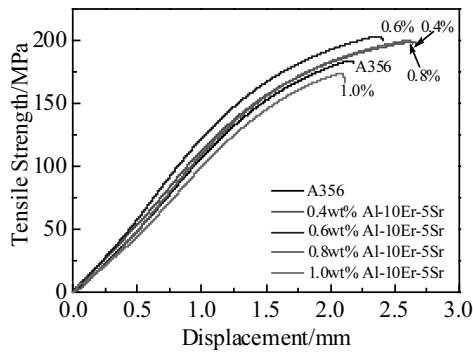


Fig.6 Tensile strength of the A356 alloys treated by different processes at as-cast state

**Table 2 Mechanical properties of the as-cast A356 aluminum alloys under different conditions**

Alloy	Master alloy	Tensile strength/MPa	Increment in UST/%
A356	0.6wt% Al-10Er-5Sr	203.5	10.7
A356.2[23]	0.2%Al5Ti1B+0.2%Al-10Sr	200.4	7.9
A356[24]	2.5%TiB <sub>2</sub> +0.1%La	187.6	10.2
A356[24]	2.5%TiB <sub>2</sub>	180.1	7.8
A356[21]	0.3%Er	195.3	5.6
A356[25]	0.6%Al-2.5Ti-0.5B-5Sr	194	7.8

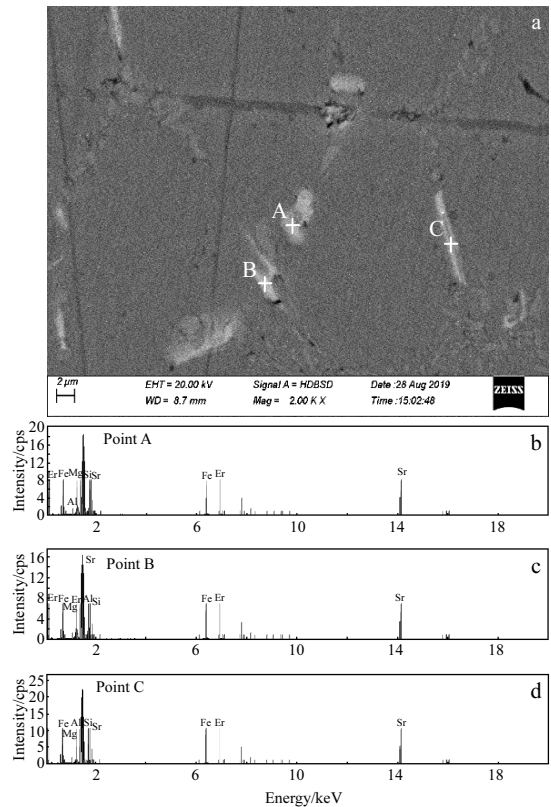


Fig.7 SEM image (a) of the A356 alloy treated by 1.0% Al-10Er-5Sr and the EDS spectra of points A (b), B (c), C (d) in Fig.7a

**Table 3 EDS analysis results of phase composition at points marked in Fig.7a (at%)**

Point	Al	Si	Mg	Fe	Er	Sr
A	74.43	12.28	8.61	2.78	0.71	1.18
B	70.79	14.35	9.13	3.42	0.88	1.42
C	85.62	6.74	4.74	1.67	0.42	0.80

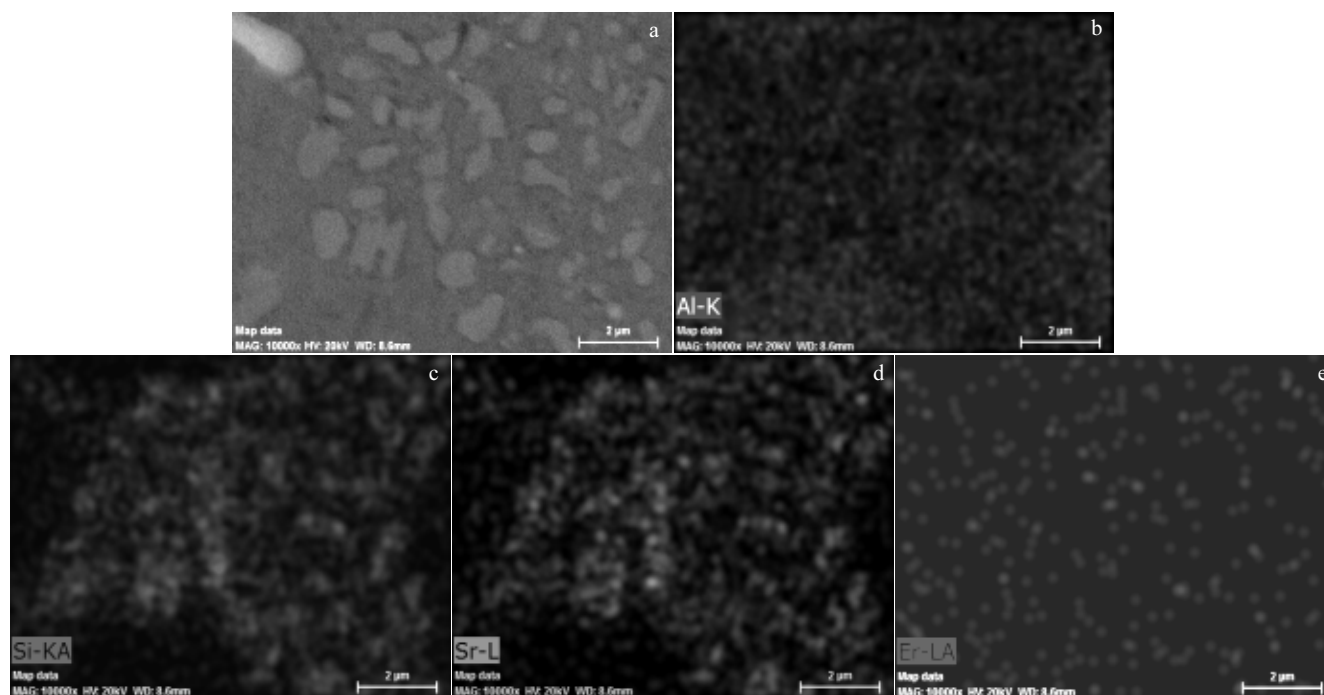


Fig.8 Area scanning results of A356 alloy treated by 0.6% Al-10Er-5Sr: (a) SE image and distribution of Al (b), Si (c), Sr (d) and Er (e)

mance are due to the combing effect of Sr and Er.

Besides, it should be noted that Er distributes uniformly in the matrix (as shown in Fig.8) and Er atom is larger than Al atom, leading to the distortion of Al lattice and the formation of the elastic stress fields, which will interact with the elastic stress fields of the dislocation. Accordingly, the resistance to dislocation movement increases and the solid solution strengthening is acquired, which finally helps to improve tensile strength.

### 3 Conclusions

1) Al-10Er-5Sr master alloy with a strip-like microstructure can be successfully fabricated by using Al-10Er and Al-10Sr master alloys. Al-10Er-5Sr master alloy is mainly composed of  $\alpha$ -Al,  $Al_4Sr$  and  $Al_3Er$  phases.

2) The addition of Al-10Er-5Sr master alloy can not only decrease the SDAS, but also modify the eutectic silicon from acicular-like to fibrous or particles. The optimal Al-10Er-5Sr content is 0.6wt%, leading to the tensile strength improvement by 10.7% compared with the traditionally treated alloys.

3) The modification mechanism of Er is similar to that of Sr. The restriction of the Si growth and optimization of eutectic silicon morphology are achieved by the combing effect of Er

and Sr.

### References

- 1 Sebaie O E, Samuel A M, Samuel F H et al. *Materials Science and Engineering A*[J], 2008, 486(1-2): 241
- 2 Faraji M, Katgerman L. *Micron*[J], 2010, 41(6): 554
- 3 Li Qinglin, Li Fubin, Xia Tiandong et al. *Journal of Alloys and Compounds*[J], 2015, 627(5): 352
- 4 Zhu M, Jian Z Y, Yang G C et al. *Materials & Design*[J], 2012, 36: 243
- 5 Wu Y P, Wang S J, Li H et al. *Journal of Alloys and Compounds* [J], 2009, 477: 139
- 6 Fan Songjie, He Guoqiu, Liu Xiaoshan et al. *Nonferrous Metals* [J], 2008, 60(4): 5 (in Chinese)
- 7 Zhang Yu, Wang Yuxin, Liao Wenjun et al. *Metallic Functional Materials*[J], 2010, 17(3): 86 (in Chinese)
- 8 Knuutinen A, Nogita K, Mcdonald S D et al. *Journal of Light Metals*[J], 2001, 1: 229
- 9 Nogita K, Yasuuda H, Yoshiya M et al. *Journal of Alloys and Compounds*[J], 2010, 489: 415
- 10 Tsai Y C, Chou C Y, Lee S L et al. *Journal of Alloys and Compounds*[J], 2009, 487: 157
- 11 Nogita K, Mcdonald S D, Dahle A K. *Materials Transactions*[J],

- 2004, 45: 323
- 12 Marzouk M, Jain M, Shankar S. *Materials Science and Engineering A*[J], 2014, 598(26): 277
- 13 Liao C W, Chen J C, Li Y et al. *Journal of Materials Science & Technology*[J], 2012, 28(6): 524
- 14 Liao H C, Huang W R, Wang Q G et al. *Journal of Materials Science & Technology*[J], 2014, 30(2): 146
- 15 Emamy M, Abdizadeh H, Lashgari H R et al. *Mechanics of Advanced Materials Structures*[J], 2011, 18(3): 210
- 16 Cui X L, Wu Y Y, Gao T et al. *Journal of Alloys and Compounds*[J], 2014, 615(5): 906
- 17 Zhao H L, Bai H L, Wang J et al. *Materials Characterization*[J], 2009, 60(5): 377
- 18 Chen X, Liu Z, Bai S et al. *Journal of Alloys and Compounds*[J], 2010, 505(1): 201
- 19 Bai S, Liu Z, Li Y et al. *Materials Science and Engineering A*[J], 2010, 527(7-8): 1806
- 20 Nie Z R, Huang H, Gao K Y et al. *Materials Science Forum*[J], 2012, 706-709: 329
- 21 Shi Z M, Wang Q, Zhao G et al. *Materials Science and Engineering A*[J], 2015, 626 (25): 102
- 22 Hu X, Jiang F, Ai F et al. *Journal of Alloys and Compounds*[J], 2012, 538(15): 21
- 23 Qiu Chuanrong, Miao Sainan, Li Xinrong et al. *Materials & Design*[J], 2017, 114(15): 563
- 24 Shabani M O, Mazahery A, Bahmani A. *Kovove Mater*[J], 2011, 49: 253
- 25 Zhao Houliang. *Study on a High Efficient Refiner and Modifier Al-Ti-B-Sr for A356 Alloy*[D]. Jinan: Shandong Jianzhu University, 2017 (in Chinese)
- 26 Wang T M, Zhao Y F, Chen Z N et al. *Materials Science and Engineering A*[J], 2015, 644(17): 425
- 27 Jiang W M, Fan Z T, Dai Y C et al. *Materials Science and Engineering A*[J], 2014, 597(12): 237
- 28 Shabani M O, Mazahery A. *Journal of the Minerals Metals & Materials Society*[J], 2011, 63(8): 132
- 29 Xing P F, Gao B, Zhuang Y X et al. *Acta Metallurgica Sinica*[J], 2010, 23: 327

## Er 和 Sr 共同作用对 A356 铝合金铸态组织和力学性能的影响

陈志强<sup>1,2</sup>, 贾锦玉<sup>2</sup>, 胡文鑫<sup>1,2</sup>, 王 玮<sup>2</sup>, 王小青<sup>1,2</sup>

(1. 包头稀土研究院 白云鄂博稀土资源研究与综合利用国家重点实验室, 内蒙古 包头 014030)

(2. 包头稀土研究院, 内蒙古 包头 014030)

**摘要:** 通过制备 Al-10Er-5Sr 中间合金并分析其微观组织和相成分, 以研究 Er 和 Sr 共同作用对 A356 铝合金微观组织和力学性能的影响。根据微观组织的发展和力学性能的变化, 确定了 Al-10Er-5Sr 中间合金在 A356 铝合金中的最佳含量。研究表明: Al-10Er-5Sr 中间合金主要由  $\alpha$ -Al, Al<sub>4</sub>Sr 和 Al<sub>3</sub>Er 相组成。A356 铝合金中加入质量分数 0.6% 的 Al-10Er-5Sr 合金后展示了最优的组织 and 力学性能, 其中合金的二次枝晶臂间距减小到 20.2  $\mu\text{m}$ , 针状共晶硅向纤维状共晶硅转变。由于微观组织的改善, 加入 0.6% 的 Al-10Er-5Sr 的 A356 合金抗拉强度提高到了 203.5 MPa, 与未添加中间合金相比, 性能明显提高。对晶粒细化和变质机理进行了分析和讨论。

**关键词:** Al-10Er-5Sr 中间合金; 变质和晶粒细化; 共同作用; 力学性能

作者简介: 陈志强, 男, 1989 年生, 硕士, 包头稀土研究院, 内蒙古 包头 014030, 电话: 0472-5179599, E-mail: 632330923@qq.com